The Astrophysical Journal Letters, 789:L22 (5pp), 2014 July 1 doi:10.1088/2041-8205/789/1/L22

PHYSICAL PROPERTIES OF NEAR-EARTH ASTEROID 2011 MD

M. Mommert[1], D. Farnocchia[2], J. L. Hora[3], S. R. Chesley[2], D. E. Trilling[1], P. W. Chodas[2], M. Mueller[4], A. W. Harris[5], H. A. Smith[3], and G. G. Fazio[3]
[1] Department of Physics and Astronomy, Northern Arizona University, P.O. Box 6010, Flagstaff, AZ 86011, USA
[2] Jet Propulsion Laboratory, California Institute of Technology, Pasadena, CA 91109, USA
[3] Harvard-Smithsonian Center for Astrophysics, 60 Garden Street, MS 65, Cambridge, MA 02138-1516, USA
[4] SRON Netherlands Institute for Space Research, Postbus 800, 9700-AV Groningen, The Netherlands
[5] DLR Institute of Planetary Research, Rutherfordstrasse 2, D-12489 Berlin, Germany
Received 2014 May 2; accepted 2014 May 29; published 2014 June 19

ABSTRACT

We report on observations of near-Earth asteroid 2011 MD with the *Spitzer Space Telescope*. We have spent 19.9 hr of observing time with channel 2 (4.5 μm) of the Infrared Array Camera and detected the target within the 2σ positional uncertainty ellipse. Using an asteroid thermophysical model and a model of nongravitational forces acting upon the object, we constrain the physical properties of 2011 MD, based on the measured flux density and available astrometry data. We estimate 2011 MD to be (6^{+4}_{-2}) m in diameter with a geometric albedo of $0.3^{+0.4}_{-0.2}$ (uncertainties are 1σ). We find the asteroid's most probable bulk density to be $(1.1^{+0.7}_{-0.5})$ g cm^{-3}, which implies a total mass of (50–350) t and a macroporosity of $\geqslant$65%, assuming a material bulk density typical of non-primitive meteorite materials. A high degree of macroporosity suggests that 2011 MD is a rubble-pile asteroid, the rotation of which is more likely to be retrograde than prograde.

Key words: infrared: planetary systems – minor planets, asteroids: individual (2011 MD)

Online-only material: color figures

1. INTRODUCTION

Little is known about the physical properties of near-Earth asteroids with diameters smaller than 100 m. Mainzer et al. (2014) measured the sizes and albedos of the smallest optically discovered near-Earth asteroids ($d > 10$ m) from NEOWISE data. Mommert et al. (2014) constrained a number of physical properties of candidate mission target 2009 BD, revealing two extraordinary but equally possible solutions.

Near-Earth asteroid 2011 MD was discovered on 2011 June 22, by the Lincoln Near Earth Asteroid Research program (Blythe et al. 2011). Five days later, the object passed Earth within a distance of 15,000 km from the surface, which significantly changed the object's orbit. 2011 MD now has a specific linear momentum (Δv), the launch velocity necessary to reach 2011 MD with spacecraft, of 4.17 km s^{-1} (L. H. Wasserman 2014, private communication), making it a very accessible candidate space-mission target asteroid. Photometric time series revealed a rotational period of (0.1939 ± 0.0004) hr with a peak-to-peak amplitude of 0.8 mag (Ryan & Ryan 2012; Warner et al. 2009). Based on its absolute magnitude ($H = 28.0 \pm 0.3$, Minor Planet Center 2014; JPL Horizons 2014; Micheli & Tholen 2014), the apparent magnitude of an asteroid at 1 AU from the Sun and the observer at a solar phase angle of zero, and assuming a most probable albedo range of 0.03–0.50, its possible diameter ranges between 4 and 22 m.

2011 MD is a potential candidate for NASA's proposed Asteroid Robotic Redirect Mission (ARRM; NASA Asteroid Initiative Website 2014; Mazanek et al. 2013). One of the proposed mission concepts for ARRM involves capturing an asteroid less than ~10 m in size and guiding it into orbit about the Moon, where it could be visited and explored by astronauts. Candidate asteroids for this concept could have masses in the range of tens to hundreds of metric tons, but the maximum mass for each candidate would depend on its orbital parameters. The size and mass of 2011 MD were not known accurately enough to determine whether it could be considered a more serious candidate for the proposed mission.

We utilize observations obtained by the *Spitzer Space Telescope* to constrain the physical properties of 2011 MD.

2. *SPITZER* OBSERVATIONS AND DATA REDUCTION

We observed 2011 MD with the Infrared Array Camera (IRAC; Fazio et al. 2004) on board the *Spitzer Space Telescope* (Werner et al. 2004) in Program ID 10132 using a total of 19.9 hr of observation time. Observations (astronomical observation request 49716480) started on 2014 February 11, 20:30:47 UT, using the "Moving Single" object mode to track in the moving frame of the object. We performed the observations in full array mode with 100 s frames in IRAC channel 2 (4.5 μm) only, using a medium cycling dither pattern with 227 dither positions and three repeats, resulting in a total of 681 frames, or 18.3 hr on-source exposure time.

At the time of the observations, 2011 MD was 1.09 AU from the Sun and 0.14 AU from *Spitzer* with a solar phase angle of 54°. The observation window was selected based on *Spitzer* observing constraints.

The data were reduced using the method by Mommert et al. (2014). A mosaic of the field is constructed from the data set itself and then subtracted from the individual basic calibrated data (BCD) frames. After subtraction of the background mosaic, residual background sources and bright cosmic ray artifacts are masked in the individual BCDs before being mosaicked in the reference frame of the moving object.

In the final co-move map we find a source within 2σ of the expected position of 2011 MD (see Figure 1, and Sections 5 and 3 for a discussion). We identify this source as 2011 MD and derive a flux density of (0.60 ± 0.27) μJy. The uncertainty is derived as the standard deviation of the photometry of implanted

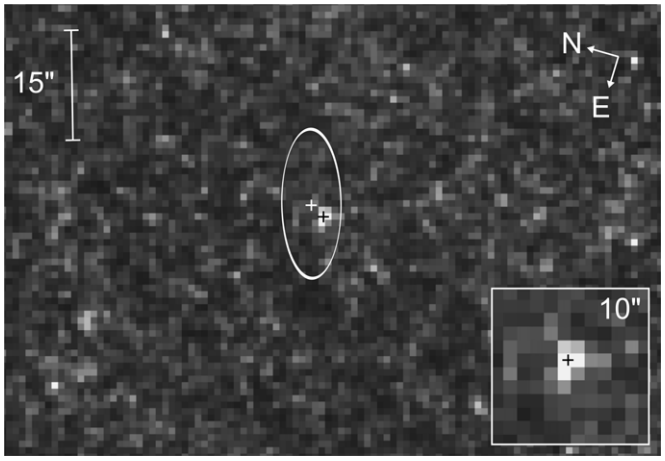

Figure 1. IRAC channel 2 (4.5 μm) map centered and stacked in the co-moving frame of 2011 MD, using a power-law color table scaling. The object's position (black cross) lies within 1σ in R.A. and 2σ in decl. of the predicted position (white cross). The white ellipse depicts the 3σ positional uncertainty. We derive a flux density and 1σ uncertainty of (0.60 ± 0.27) μJy. The inset shows a $10'' \times 10''$ postage stamp of 2011 MD.

fake sources with flux densities of 0.6 mJy into various positions of the co-move map.

3. MODELING

We constrain the physical properties of 2011 MD by combining an asteroid thermophysical model with a model of the nongravitational forces acting on the asteroid, similar to the approach taken by Mommert et al. (2014).

The thermophysical model approximates the surface temperature distribution of 2011 MD and is used to determine the thermal-infrared emission from its surface as a function of its physical properties, including spin axis orientation (represented by the obliquity, γ), rotational period, P, thermal inertia, Γ, and surface roughness. Surface roughness causes infrared beaming, an effect that focuses thermal emission radiated toward the observer, and is modeled as emission from spherical craters (see Mueller 2007 for more details). The model solves the heat transfer equation numerically for a large number of plane surface facets that form a sphere. The model we use is nearly identical to the one used by Mueller (2007). Since the single-band nature of our observation precludes a direct fit of the target's spectral energy distribution, we take a probabilistic approach in which we explore the parameter space by varying the individual input parameters.

Similar to Mommert et al. (2014), we model the nongravitational acceleration of the object as a result of the solar radiation pressure (using the approach by Vokrouhlický & Milani 2000) and the Yarkovsky force (Vokrouhlický et al. 2000). The model asteroid is assumed to be spherical and the heat transfer is solved analytically using the linearized heat transfer equation (Vokrouhlický 1998; Vokrouhlický & Farinella 1999). By fitting all available astrometric data of 2011 MD, the model derives the bulk density, ρ, and the goodness-of-fit parameter χ^2 as a function of the asteroid's properties.

Ground-based astrometric observations of 2011 MD cover the date range 2011 June 21 to 2011 September 3 (1555 observations) in addition to our *Spitzer* detection (2014 February 11). The majority of the observations were collected during the close Earth encounter of 2011 June. Of special importance for the deductions made in this work are the astrometric measurements performed by Micheli & Tholen (2014), which extend the observed arc until 2011 September. We model the nongravitational perturbations as

$$\mathbf{a}_{\rm NG} = (A_1\hat{\mathbf{r}} + A_2\hat{\mathbf{t}}) \left(\frac{1\ {\rm AU}}{r}\right)^2, \quad (1)$$

where $\hat{\mathbf{r}}$ and $\hat{\mathbf{t}}$ are the radial and transverse directions, respectively, and r is the heliocentric distance. A_2/r^2 translates into the transverse component of the Yarkovsky effect (Bottke et al. 2006), whereas A_1/r^2 models the solar radiation pressure and the radial component of the Yarkovsky effect. We use this simplified model approach for ephemeris predictions and to investigate the detectability of nongravitational forces in the astrometric data. In order to fit the model to the astrometric data, we applied the Chesley et al. (2010) debiasing and weighting scheme. Since timing errors are more relevant when an object is observed at small geocentric distances, we relaxed the data weights for these observations. In the case of our *Spitzer* observations, we applied an uncertainty of $1''$, accounting for the positional uncertainty of 2011 MD from our observation and the uncertainty of *Spitzer*'s ephemeris (J. Lee & T. J. Martin-Mur 2014, private communication). The orbital fit (JPL Solution 40) to the observations yields $A_1 = (7.21 \pm 2.26) \times 10^{-11}$ AU d^{-2} (3.4σ confidence) and $A_2 = (-1.13 \pm 2.91) \times 10^{-12}$ AU d^{-2} (0.4σ). Our value of A_1 agrees within uncertainties with the value found by Micheli & Tholen (2014) ($A_1 = (7.3 \pm 1.4) \times 10^{-11}$ AU d^{-2}, 5.2σ). We ascribe our higher uncertainty to a less strict weighting used for some of the available astrometric data, and the fact that we have taken into account the Yarkovsky effect (A_2), which was neglected by Micheli & Tholen (2014), and leads to additional uncertainty, due to the correlation of A_1 and A_2.

4. RESULTS

We explore the physical property space of 2011 MD based on our flux density measurement, using a Monte Carlo method in which we generate 40,000 randomized synthetic objects. We sample the rotation period $P = (0.1939 \pm 0.0004)$ hr (Ryan & Ryan 2012; Warner et al. 2009), the absolute magnitude $H = 28.0 \pm 0.3$ (Micheli & Tholen 2014), and the photometric slope parameter $G = 0.18 \pm 0.13$ (average from all G measurements of asteroids; see JPL Small-Body Database Search Engine 2013), using normal distributions. Due to the lack of observational constraints, we uniformly sample the physically meaningful ranges in thermal inertia (10–5000 SI units, where 1 SI unit equals 1 J m^{-2} s$^{-0.5}$ K^{-1}), the azimuth of the spin axis orientation and the cosine of the obliquity (covering $\gamma = 0$–180°, sampling the cosine leads to a truly random distribution of the spin vector), and use various surface roughness models (see, Mueller 2007). We draw flux densities from a normal distribution with a mean of 0.6 μJy and a 1σ uncertainty of 0.27 μJy (we reject negative flux densities). For each set of input parameters, the diameter and albedo are derived by fitting the thermophysical model flux density to a randomized flux density. The resulting diameters and albedos, as well as the input parameters of the thermophysical model are then used in the orbital model in order to derive ρ and χ^2 for each synthetic object. The final distributions in diameter, albedo, obliquity, and density are weighted using χ^2 from the orbital fit in order to account for the compatibility with the astrometric data. Other parameters, such as H, G, and Γ, are not sensitive to χ^2.

We reject synthetic model asteroids with unphysically high Bond albedos. The Bond albedo, A, describes the reflectivity

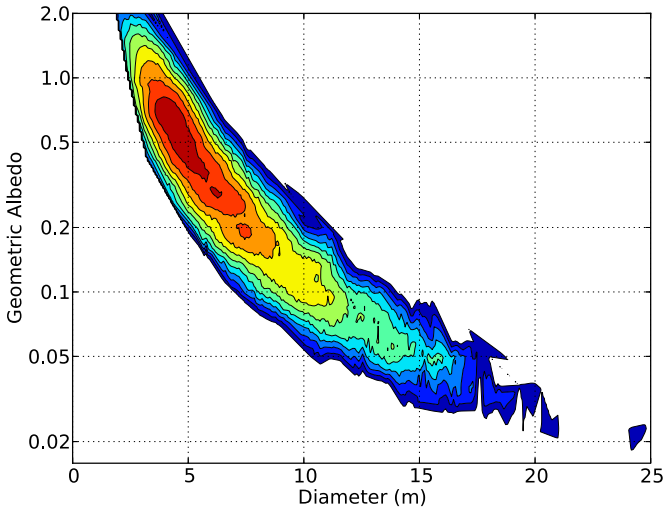

Figure 2. Distribution of the 40,000 synthetic model asteroids generated in the Monte Carlo method in albedo-diameter space. Contour lines and colors represent the logarithm of the weighted number density of synthetic model asteroids per space element. The median of the distributions in diameter and albedo is 6 m and 0.3, respectively.

(A color version of this figure is available in the online journal.)

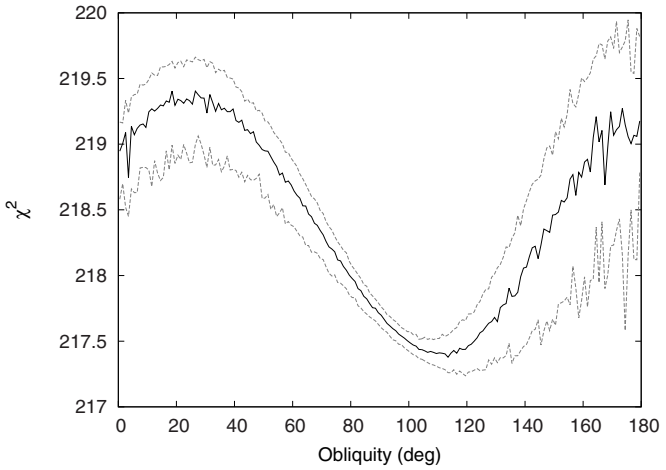

Figure 3. Orbital model χ^2 distribution as a function of obliquity as derived from the Monte Carlo method. The continuous black line represents the median per bin in obliquity; dashed gray lines indicate the 1σ confidence interval. The distribution shows a global minimum at $\sim$110°, favoring a retrograde rotation of 2011 MD.

integrated over the whole electromagnetic spectrum and can be approximated as $A \sim q \cdot p_v$, with the phase integral $q = 0.290 + 0.684 \cdot G$ (Bowell et al. 1989). Hence, high geometric albedos p_V can lead to $A > 1$, which contradicts the law of conservation of energy.

The final results of our analysis are depicted in Figures 2–4 and show that 2011 MD has a mean diameter of (6^{+4}_{-2}) m (1σ) and an albedo of $0.3^{+0.4}_{-0.2}$ (1σ). Note that in the case of asymmetric uncertainties, the 1σ confidence interval refers to the 68.3% of values higher/lower than the median value. The 3σ confidence interval covers a range of (2–26) m in diameter and $\geqslant$0.02 in albedo. From the orbital model we find a most probable bulk density of $(1.1^{+0.7}_{-0.5})$ g cm^{-3} (1σ, 3σ interval: (0.2–5.0) g cm^{-3}), which translates into a total mass of (110^{+240}_{-60}) t (1σ, 3σ interval: (10–2500) t). The measured albedo is compatible with a number of non-primitive taxonomic classes (Thomas et al. 2011).

Our model results favor a retrograde rotation of 2011 MD, which is suggested by the χ^2 distribution produced by the orbital model (see Figure 3), or the negative value of A_2 (compare to Farnocchia et al. 2013). Note that in case of a complex rotation of the object, our definition of obliquity is referenced to the rotational angular momentum vector rather than the spin axis. We are unable to constrain the thermal inertia of 2011 MD, given the low confidence in the measurement of A_2.

5. DISCUSSION

Figure 1 depicts the 3σ positional uncertainty of 2011 MD during our observations as an ellipse with semimajor axes 9.″9 and 3.″9 at an angle of 163° (east to north). The uncertainty is based on all available ground-based astrometric data, physically reasonable values of A_1 and A_2, as well as *Spitzer* ephemeris and astrometric image calibration uncertainties. The position of the source associated with 2011 MD agrees within less than 2σ with the expected position of 2011 MD and has the highest signal-to-noise ratio in the co-move map. The appearance of the source agrees with the IRAC point-spread function, which has a FWHM of 1.″66 (1.4 pixel). Figure 1 shows that potential sources other than 2011 MD are constrained to only one high-signal pixel. We investigated the possibility that the source we identify as 2011 MD is a product of noise. For this reason, we created co-move maps from the BCDs with rates that are close, but not identical, to the rate of 2011 MD. This approach precludes an alignment of the positions of 2011 MD in the co-move maps, which have noise properties on both large and small scales that are nearly identical to those of the original co-move map. We identified potential sources within 1′ of the image center in each map and compared their flux densities with the measurements from the original co-move map showing 2011 MD. In a total of 1000 co-move maps, we found the brightest source to have a signal that is 20% lower than that measured for 2011 MD; only 0.01% of all potential sources have flux densities that are 20–30% lower than the flux density measured for 2011 MD. The probability that the source we identify as 2011 MD is a noise feature and falls within the 3σ error ellipse is $\leqslant 5 \times 10^{-6}$. Further note that individual BCDs were aligned in the moving frame of 2011 MD. During the observations, 2011 MD covered a distance of $\sim$16.′6 (>3 IRAC fields of view), basically ruling out the possibility that the source is a background object or a moving object on an orbit different than that of 2011 MD. Hence, we are confident that we correctly identified 2011 MD.

The model approach used in this work is identical to the one used by Mommert et al. (2014). Both the thermophysical and the orbital model have been tested extensively and compared to other models. We take this Monte Carlo approach in order to minimize the number of *a priori* assumptions on the properties of 2011 MD; e.g., we do not preclude high albedos. We allow for albedo up to values where the Bond albedo reaches unity (see Section 4). Restricting the upper-limit further to values that have been observed in other asteroids ($p_V < 1.0$, see, e.g., Thomas et al. 2011; Mainzer et al. 2011) changes our model results only slightly and we find a most probable diameter of 6.2 m and a bulk density of 1.0 g cm^{-3}. Note that these values are well within the 1σ confidence intervals of our nominal model solutions.

The wide range of possible albedos precludes a rough taxonomic classification of 2011 MD. However, it is very unlikely that 2011 MD is a primitive asteroid type with an albedo less than 0.1; the probability for $p_V \leqslant 0.1$ is only 5%. Assuming 2011 MD to consist of material comparable to ordinary chondrites, which has the lowest density of all

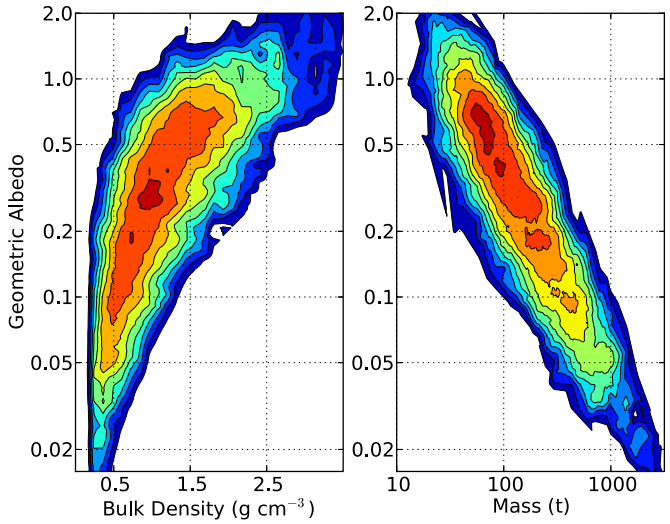

Figure 4. Bulk density (left) and total mass (right) distributions of the synthetic model asteroids, weighted with the orbital model χ^2 (see Figure 2 for definitions). Both parameters are a strongly correlated to albedo. We adopt the median of each weighted distribution, yielding a most probable bulk density of $(1.1^{+0.7}_{-0.5})$ g cm^{-3} and total mass of (110^{+240}_{-60}) t.

(A color version of this figure is available in the online journal.)

non-primitive materials, we can derive a lower limit on the macroporosity of this object of 65% (see, Mommert et al. 2014; Britt et al. 2002). This high degree of macroporosity suggests a rubble-pile nature for 2011 MD, which is possible despite its fast rotation (Scheeres et al. 2010).

Our bulk density estimate (1.1 g cm^{-3}) is nearly twice as high as the value found by Micheli & Tholen (2014). This difference is caused by their neglect of Yarkovsky forces and the assumption that 2011 MD's albedo follows the albedo distribution for small ($10 < d < 100$ m) asteroids (Mainzer et al. 2014). Using the same assumptions, our results are consistent (M. Micheli 2014, private communication). Figure 4 plots bulk density and total mass as a function of albedo, both of which show a strong dependence on albedo.

We compare the physical properties of 2011 MD with those found for other small asteroids. In comparison to the extraordinary solutions for 2009 BD (Mommert et al. 2014), 2011 MD is slightly larger (diameter of 2009 BD: 2.9 m or 4.0 m), has a lower density (higher macroporosity) than either solution ($\rho = 2.9$ g cm^{-3} or $\rho = 1.7$ g cm^{-3}), and has a more moderate albedo ($p_V = 0.85$ or $p_V = 0.45$). The albedo measured for 2011 MD is compatible with the albedo distribution of 10–100 m sized asteroids found by Mainzer et al. (2014). The bulk density and macroporosity of 2011 MD are comparable to values observed in some asteroids larger than 100 m (see Mommert et al. 2014).

Note that the diameter derived as part of this work is the effective diameter of a sphere with the same volume as the real shape of 2011 MD. The large lightcurve amplitude of 0.8 mag (Ryan & Ryan 2012), however, suggests a highly elongated shape of 2011 MD with an axis ratio of $b/a \sim 0.5$, where (a,b,c) are the axes of a triaxial ellipsoid. The rotational period of 0.1939 hr (Ryan & Ryan 2012) is significantly shorter than our observation duration (19.9 hr); any optical lightcurve effects are hence averaged over our observation. We investigate the impact of the temperature distribution of an ellipsoid with an axis ratio similar to that of 2011 MD compared to that of a sphere. We use a simplistic model of the shape of 2011 MD that is based on a triaxial ellipsoid with axis ratio (1,0.5,0.5); since there is no information on the c axis, we assume $c = 0.5$, which provides a principal axis rotation of the body. We approximate the measured lightcurve of 2011 MD with a step function: the observer is faced the long side of the asteroid ($a \times c$) for 75% of the rotation period and the short side ($b \times c$) for the remaining 25% (compare with Figure 2 by Ryan & Ryan 2012). We realize this lightcurve behavior by using a composite flux density that consists to 75% of the flux density emitted by the long side and to 25% of the flux density emitted by the short side. We compare the diameter derived with this composite flux density with that of a spherical shape and find differences up to 20%, depending on the spin axis orientation and thermal inertia. This uncertainty, which is based on a coarse approximation of the real shape of 2011 MD, is well within the nominal 1σ diameter uncertainties used in our model approach. Also, the assumed ellipsoidal shape has a cross section that is different from that of a spherical shape, which affects the solar radiation pressure acting on the object, and hence changes its bulk density. We find that the average cross section of the ellipsoid is 10% larger than that of a sphere, forcing the same change in bulk density. Again, the nominal uncertainty in bulk density is significantly larger than this change.

Our observations have provided a determination of the physical properties of 2011 MD, and in particular, its size and mass. A final evaluation of 2011 MD as a candidate target for the proposed ARRM mission is beyond the scope of this work.

Some of the computational analyses were run on Northern Arizona University's monsoon computing cluster, funded by Arizona's Technology and Research Initiative Fund. M. Mommert thanks P. Penteado for support on the computational aspects of this work. We thank J. Lee and T. J. Martin-Mur for providing information on the *Spitzer* ephemeris uncertainties. We thank an anonymous referee for useful suggestions that led to the improvement of this manuscript. The work of D. Farnocchia, S. Chesley, and P. W. Chodas was conducted at the Jet Propulsion Laboratory, California Institute of Technology under a contract with the National Aeronautics and Space Administration. J. L. Hora and H. A. Smith acknowledge partial support from Jet Propulsion Laboratory RSA #1367413. This work is based on observations made with the *Spitzer Space Telescope*, which is operated by the Jet Propulsion Laboratory, California Institute of Technology under a contract with NASA.

Facility: Spitzer

REFERENCES

Blythe, M., Spitz, G., Brungard, R., et al. 2011, MPEC, 2011-M23
Bottke, W. F., Vokrouhlický, D., Rubincam, D. P., & Nesvorný, D. 2006, AREPS, 34, 157
Bowell, E., Hapke, B., Domingue, D., et al. 1989, in Asteroids II, ed. R. P. Binzel, T. Gehrels, & M. S. Matthews (Tucson, AZ: Univ. Arizona Press), 524
Britt, D. T., Yeomans, D., Housen, K., & Consolmagno, G. 2002, in Asteroids III, ed. W. F. Bottke Jr., A. Cellino, P. Paolicchi, & R. P. Binzel (Tucson, AZ: Univ. Arizona Press), 485
Chesley, S. R., Baer, J., & Monet, D. G. 2010, Icar, 2010, 158
Farnocchia, D., Chesley, S. R., Vokrouhlický, D., et al. 2013, Icar, 224, 1
Fazio, G. G., Hora, J. L., Allen, L. E., Ashby, M. L. N., & Barmby, P. 2004, ApJS, 154, 10
JPL Horizons System. 2014, http://ssd.jpl.nasa.gov/horizons.cgi#top, accessed 2014 March 11
JPL Small-Body Database Search Engine. 2013, http://ssd.jpl.nasa.gov/sbdb_query.cgi, accessed 2013 October 28
Mainzer, A., Bauer, J., Grav, T., Masiero, J., & Cutri, R. M. 2014, ApJ, 784, 110

Mainzer, A., Grav, T., Bauer, J., Masiero, J., & McMillan, R. S. 2011, ApJ, 743, 156
Mazanek, D. D., Brophy, J. R., & Merrill, R. G. 2013, in IAA Planetary Defense Conf. (Paris: IAA), http://ntrs.nasa.gov/archive/nasa/casi.ntrs.nasa.gov/20130013170.pdf
Micheli, M., & Tholen, D. J. 2014, ApJL, 788, L1
Minor Planet Center Database. 2014, http://www.minorplanetcenter.net/db_search, accessed 2014 April 10
Mommert, M., Hora, J. L., Farnocchia, D., Trilling, D. E., & Chesley, S. R. 2014, ApJ, 786, 148
Mueller, M. 2007, PhD thesis, Freie Universität Berlin
NASA Asteroid Initiative Website. 2014, http://www.nasa.gov/mission_pages/asteroids/initiative/index.html, accessed 2014 March 11
Ryan, E. V., & Ryan, W. H. 2012, in Advanced Maui Optical and Space Surveillance Technologies Conference, http://www.amostech.com/TechnicalPapers/2012/Astronomy/RYAN.pdf, accessed 2014 April 4
Scheeres, D. J., Hartzell, C. M., Sánchez, P., & Swift, M. 2010, Icar, 210, 968
Thomas, C. A., Trilling, D. E., Emery, J. P., Mueller, M., & Hora, J. L. 2011, AJ, 142, 85
Vokrouhlický, D. 1998, A&A, 335, 1093
Vokrouhlický, D., & Farinella, P. 1999, AJ, 118, 3049
Vokrouhlický, D., & Milani, A. 2000, A&A, 362, 746
Vokrouhlický, D., Milani, A., & Chesley, S. R. 2000, Icar, 148, 118
Warner, B. D., Harris, A. W., & Pravec, P. 2009, Icar, 202, 134
Werner, M. W., Roellig, T. L., Low, F. J., Rieke, G. H., & Rieke, M. 2004, ApJS, 154, 1